Engineering Applications of Computational Fluid Mechanics Vol. 6, No. 2, pp.203–213 (2012)

EFFECT OF COMBUSTOR GEOMETRY ON PERFORMANCE OF AIRBLAST ATOMIZER UNDER SUB-ATMOSPHERIC CONDITIONS

N. Grech, A. Mehdi, P. K. Zachos *, V. Pachidis and R. Singh

Cranfield University, School of Engineering, Department of Power and Propulsion, Gas Turbine Performance Engineering Group, Cranfield, Bedfordshire, MK43 0AL,UK
** E-Mail: p.zachos@cranfield.ac.uk (Corresponding Author)*

ABSTRACT: One of the certification requirements that a jet engine has to fulfil is its altitude relight capability. Relighting an aero gas turbine engine at high altitudes is more challenging than at sea level conditions. The pressure, air velocity, and temperature within the combustor at such conditions are very low, hindering the fuel atomization and evaporation process. After ignition, combustion efficiency can be relatively low due to the poor fuel atomization quality, leading to slow shaft acceleration rates. Further studies in this field can help determine and predict the fuel spray characteristics, which limit the relight and pull-away capability of the engine at these sub-idle conditions. Reported in this paper is the CFD analysis of a typical airblast atomizer, simulated at different sub-idle operating conditions. Two sets of models were used; one with a simple liner-only combustor with co-flow air, and the other with a more detailed geometry, including wall cooling slots, primary and secondary dilution holes, and co-flow air. For the simpler model, three different inner and outer liner wall spacing were modelled to examine the effect of the chamber volume on the fuel spray behaviour. The CFD models were then run at a chamber pressure of 101, 41 and 31kPa, typical of sub-idle conditions. The effect of such conditions on the atomization quality of the fuel spray was analysed. The study carried out indicates how the chamber pressure, chamber volume and AFR (through amount of co-flow air introduced) significantly affect the resulting spray characteristics. A parametric analysis was performed to extract a correlation between the spray SMD (Sauter Mean Diameter) and fuel flow rate.

Keywords: airblast atomiser, evaporation, spray, sub-atmospheric

1. INTRODUCTION

Prediction of the relight and pull-away capability of a modern aero gas turbine combustor, after a flame-out at high altitude, is still a challenging field. As new modern high bypass turbofan engines are designed for better efficiency, SFC, quick and reliable ignition and low emissions, combustor design is becoming increasingly important and difficult.

An in-flight shutdown can occur due to an engine malfunction, external factors (such as volcanic ash) or a deliberate shutdown by the pilot. However, for each scenario, the chamber conditions (temperature, pressure and air velocity), chamber volume, and spray characteristics (Datta and Som, 1999; Lefebvre, 1985; Lefebvre, 1998) greatly determine the relight and pull-away capability of the engine.

A useful unit of measurement in terms of spray quality is the Sauter Mean Diameter (SMD), defined as the droplet diameter which has the same volume to surface area ratio as that of the whole spray.

The lower the SMD, the easier it is for a droplet to evaporate since it has a large surface area in relation to the volume of fluid it contains. Small values of SMD give higher values of combustion efficiency as pointed out by Lefebvre (1985, 1989 and 1998), using equation 1.

$$\eta_{ce} = 1 - exp\left[\frac{-36 \times 10^{-6} P_3 V_c \lambda_{eff}}{T_c SMD^2 f_c \dot{m}_A}\right] \quad (1)$$

SMD increases with a decrease in chamber pressure and relative air velocity. These conditions are typical of an altitude relight condition, and therefore combustion efficiency at these conditions is very low, hindering the pull-away capability of the engine.

Traditionally, spray characteristics are experimentally measured using atomizer test rigs. However, the increasing fidelity and reliability of numerical solvers encourages their use for studying the spray phenomena under conditions that are otherwise difficult to reproduce within an experimental environment. Examples of successful application of CFD studies can be found in Zachos et al. (2011), Manzar et al. (2009) and Chalet et al. (2010).

In this paper, results from a number of atomizer CFD simulations that were run at sub-atmospheric pressures are presented. These results indicate

Received: 30 Jun. 2011; Revised: 6 Dec. 2011; Accepted: 12 Dec. 2011

clearly the dominant effect on the spray characteristics of the chamber pressure, which has a direct effect on the air density, and AFR.

2. EXPERIMENTAL STUDIES

Under low power conditions, spray characteristics deteriorate, as demonstrated by Caines et al. (2001), Jasuja (1994, 1979 and 1984), Beck et al. (1989) and Parsons et al. (1986), leading to an increase in fuel droplet diameter. An experimental investigation by Caines et al. (2001) shows the influence of sub-atmospheric conditions (at 31 and 41kPa) on the spray, as illustrated in Fig. 1. Results show a wide broadening of the droplet size distribution and SMD when compared to idle. Since most of the fuel is within the larger droplets, the evaporation rate decreases, causing a slower combustion reaction and a reduction in combustion efficiency (Datta and Som, 1999; Lefebvre; 1985, Lefebvre, 1998).

Beck et al. (1989), as shown in Fig. 2, conducted similar experiments for conditions of low air velocity and different air/fuel ratios (AFR). The results indicate an increase in SMD with decreasing relative air velocity. This is attributed to the decrease in aerodynamic shear forces acting on the liquid sheet.

As the relative velocity approaches zero, the SMD continues to increase until a certain value is reached. The SMD remains constant at this value, even if the relative velocity is decreased further, indicating that a threshold exists below which the SMD does not increase further.

The SMD is also sensitive to the liquid mass flow rate, with SMD increasing as the liquid mass flow increases. This is because the air/liquid mass flow ratio (basically the AFR) decreases, causing the air momentum per unit mass of liquid to decrease until it is no longer capable of fracturing the fuel efficiently. SMD was also found to deteriorate with increase in liquid surface tension and viscosity.

Jasuja (1984), whose experiments, as shown in Fig. 3, demonstrated the influence of the operating pressure on the SMD for the same AFRs, made similar observations. All these points are attributed to the Weber (We) number, defined as:

$$We = \frac{\rho_A d_0 U_R^2}{\sigma} \tag{2}$$

The Weber number is a ratio between the disruptive and restorative forces acting on the droplet, which are the aerodynamic force of the air and the droplet surface tension respectively. In

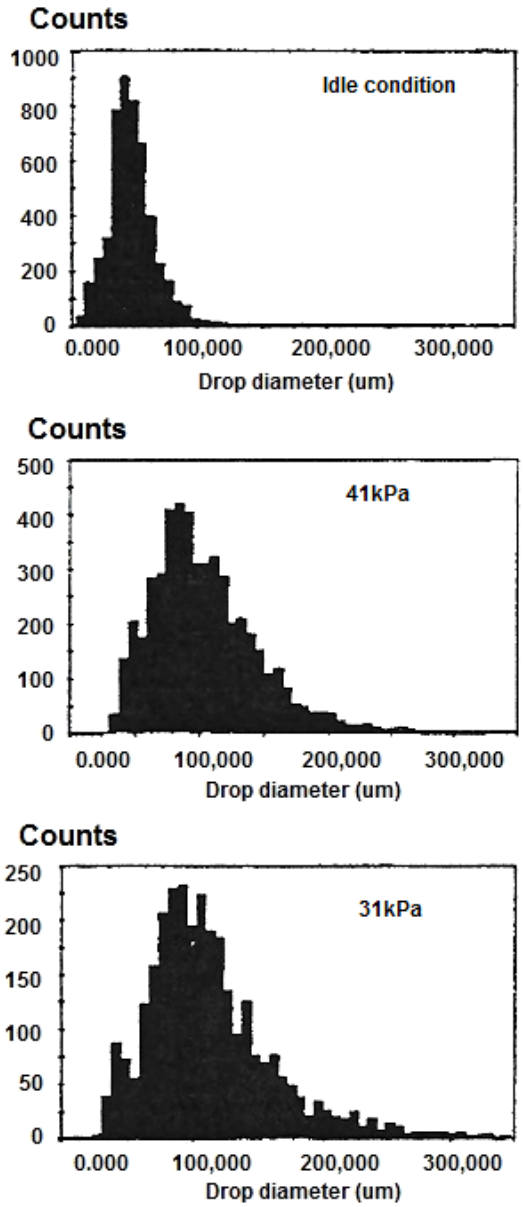

Fig. 1 Droplet sizes for various operating pressures (Caines et al., 2001).

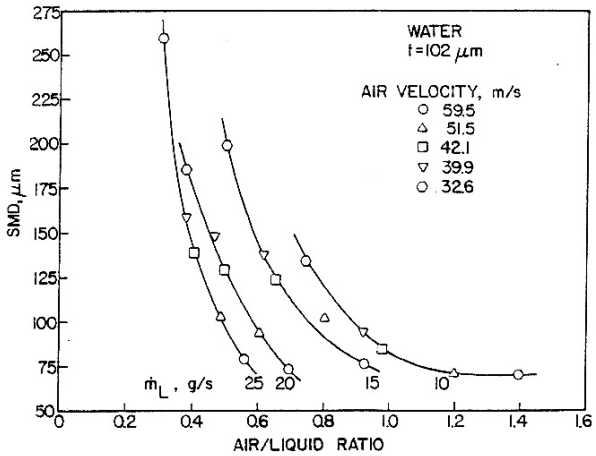

Fig. 2 Effects of AFR and air velocity on SMD (Beck et al., 1989).

order to initiate break-up, the aerodynamic force must be greater or equal to the surface tension force. Fig. 4 indicates the different break-up modes possible, depending on the Weber number. Rizkalla (1974) and Rizkalla and Lefebvre (1975) conducted a wide range of experimental studies on the effects of air and fuel properties on the atomization quality of an airblast atomizer. Results show how for liquids of low viscosity, the dominant factors are air velocity and air density; SMD being inversely proportional to both. This again points towards having a large Weber number for better atomization. This is a very significant observation, since during an altitude relight, air density will be very low, coupled with a low velocity due to the low air mass flow passing through the wind milling engine. It was also observed that liquid viscosity has an effect, which is quite separate and independent of air velocity.

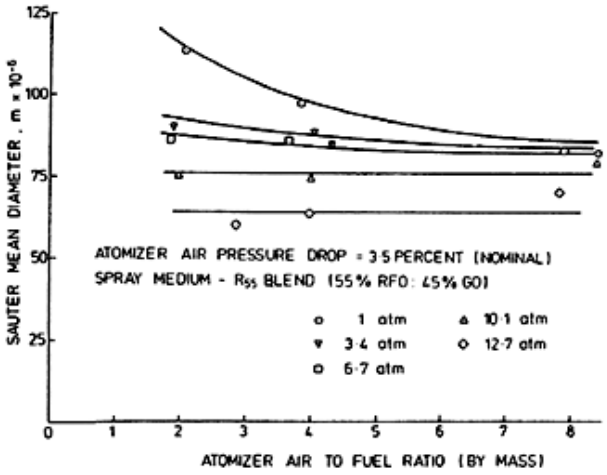

Fig. 3 Effect of AFR and operating pressure on SMD (Jasuja, 1984).

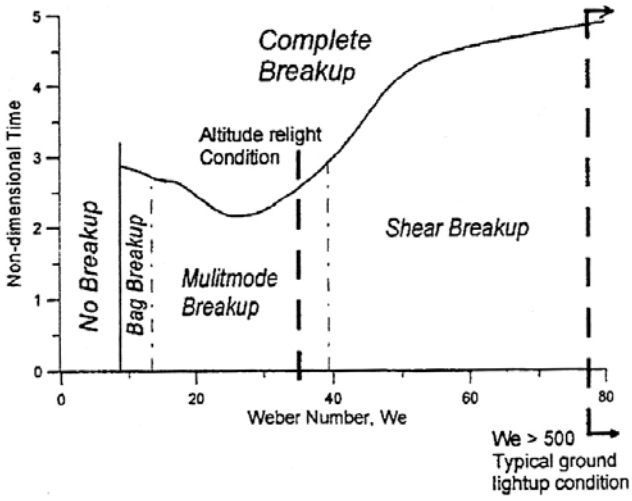

Fig. 4 Weber number with operating condition (Caines et al., 2001).

3. NUMERICAL MODEL

The airblast atomizer model used in this study has been presented in Kozaily et al. (2009). It consists of three air swirlers, all co-swirling and concentric. The fuel is also introduced in a swirling manner between the middle and the innermost air swirler (Fig. 5). For the simple combustor model (Fig. 6), the baseline spacing of the liner used is similar to that of the real engine. The other two models have half and double the spacing between the wall and the atomizer. The primary, secondary and cooling holes on the liner were not included in this model but were included in the more detailed model as shown in Fig. 7. The liner spacing for this model is similar to that of the baseline model.

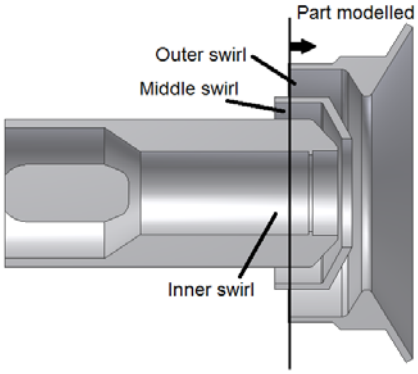

Fig. 5 Atomizer modeled – cross sectional view.

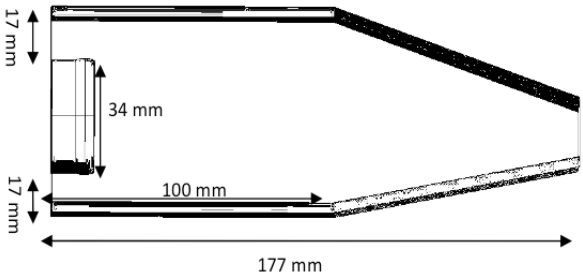

Fig. 6 Dimensions of simple combustor model (baseline spacing).

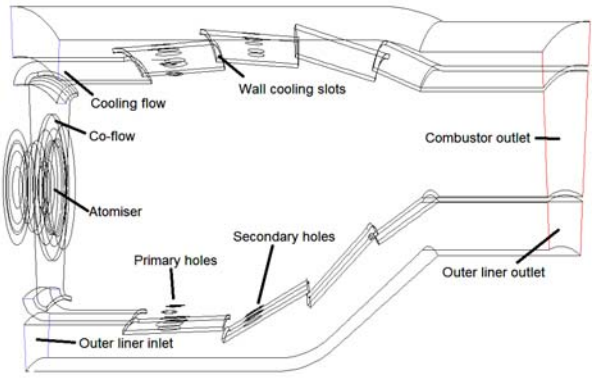

Fig. 7 Detailed combustor geometry.

3.1 Boundary and operating conditions

For both models, inlet boundaries were set as velocity inlets, with magnitudes as shown in Table 1. These values were taken from rig tests simulating combustor conditions following an engine flame-out. Outlets were set as pressure outlets with 0Pa (gauge pressure) for combustor outlet, and 500Pa (gauge pressure) for liner outlet in the detailed model. Mass flows were calculated accordingly. The domains are rotationally periodic. The air swirlers were not geometrically modelled.

The swirl components were directly introduced in the atomizer airflow using ANSYS Fluent settings. In the current studies, the vane angle was assumed to be about 45^0 and was kept constant for all the simulations. This is the typical direction of the resulting flow having equal tangential and axial components and a typical angle used in swirl atomizers. The temperature was kept constant at 300K. Air entering the model was assumed to have a 0.23 mass fraction of oxygen (assuming dry air) with its density depending on the case study at that altitude. Fuel used was typical Jet A (kerosene) aviation fuel.

Whilst both inlet air velocity and swirler outlet angles within the atomizer were kept constant for all the simulations, further studies are required to predict more accurately any changes in the atomizer flow field under such low power conditions. The air velocity within the atomizer depends on the pressure drop across it. Therefore, the 101, 41 and 31kPa cases would in fact, have different air velocities. Similarly, due to the low air mass flow through the swirlers, the flow outlet angle (and therefore the flow field) may be different from the vane angle, especially if Reynolds numbers are very low, as described by Sheen et al. (1996).

In order to predict such behaviour, one needs to predict the pressure drop across the atomizer at different engine sub-idle operating conditions. This can be done through a specialised code, or through CFD by modelling the combustor from a further upstream position, e.g. the diffuser.

Furthermore, the swirlers have to be tested / simulated with a low mass flow and at low pressure conditions to evaluate whether the flow behaves differently as it exits the swirlers. Such studies are being carried out by the authors to improve the accuracy of the combustor model.

3.2 Grid sensitivity analysis

A grid sensitivity analysis was carried out to choose the grid size which delivers the best compromise between CPU time and accuracy. This resulted in 1.7 million cells for the simple geometry. 2.2 million cells were used for the detailed geometry, after applying the same mesh density as the simple geometry case.

Meshing was accomplished using Gambit meshing software with a tri cooper mesh, including a refined tri pave mesh near the atomizer. A typical cell size of 0.5mm near the injector was chosen to make the cell smaller than the pre-filmer diameter.

The selection of the grid size was based on the accuracy of the solver in predicting the axial and tangential velocity of the swirling slow at the atomizer exit plane. Readings were taken radially. As shown in Figs. 8 and 9, the solution remains unchanged between the 1.7 million and 2.0 million cell simulations.

Table 1 Inlet velocity magnitudes.

Boundary inlet velocities [m/s]	
Inner swirl air	69
Dome swirl air	30
Middle swirl air	30
Remaining air inlets	18.5

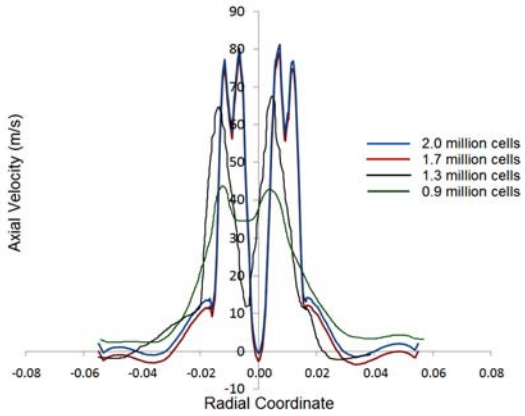

Fig. 8 Axial velocity profile for different mesh sizes.

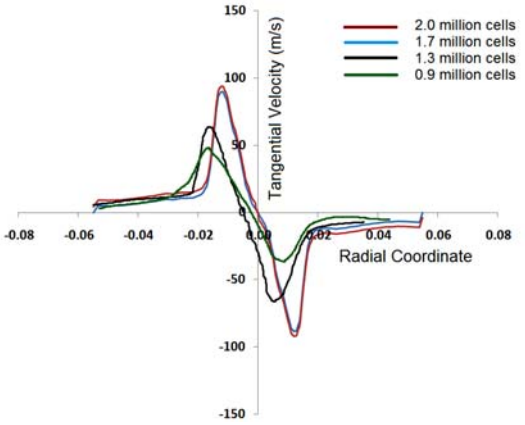

Fig. 9 Tangential velocity profile for different mesh sizes.

3.3 Numerical models

The solver was set to use the incompressible Reynolds-Averaged Navier-Stokes (RANS) equations along with the Lagrangian Discrete Phase Model (DPM) equations to determine the fuel secondary breakup process and droplet position (Reitz, 1987). The turbulence model used is the RNG k-ε two-equation model. Details concerning these modelling methods are also described by Gjesing et al. (2009) and Datta and Som (1999) with respect to spray CFD modelling. Steady simulations were run for the 1st order solution, which was then used to run 2nd order unsteady simulations for the continuous phase. Unsteady discrete phase simulations were run using the unsteady 2nd order continuous phase simulation solutions.

3.3.1 Lagrangian model

The Lagrangian (Euler-Lagrange) technique considers the discrete phase model as spherical droplets within a continuum fluid (gas phase). This model calculates the trajectory of each particle by integrating Newton's second law within a Lagrangian reference frame (Rizkalla and Lefebvre, 1975).
Lagrangian equation of motion:

$$\frac{du_p}{dt} = F_D\left(u - u_p\right) + \frac{g_x\left(\rho_p - \rho\right)}{\rho_p} + F_x \tag{3}$$

where:

$$F_D = \frac{18\mu}{\rho_p d_p^2}\frac{C_D Re}{24} \tag{4}$$

$$Re \equiv \frac{\rho d_p \left|u_p - u\right|}{\mu} \tag{5}$$

An alternative method is the Eulerian (Euler-Euler) technique, which however is unable to track particle trajectories, therefore considered unsuitable for the current study. The Lagrangian Discrete Random Walk (DRW) model is used to account for the effect of the gas-phase turbulence on the discrete phase (Tu, 2008). The solver provides two tracking models:

1. Stochastic tracking: were the solver predicts the turbulent dispersion of particles by integrating the trajectory equations for individual droplets using the instantaneous fluid velocity.
2. Particle cloud tracking: turbulent dispersion of particles about a mean trajectory is calculated using statistical methods.

Due to the cloud model not being available for unsteady particle tracking, the stochastic model was selected.

3.3.2 RANS RNG k-ε turbulence model

The RNG k-ε model is derived using the *renormalization group theory* statistical technique. It is similar to the standard k-ε model, but has a number of refinements, which make it more accurate and reliable than standard k-ε.
It is derived from the instantaneous Navier-Stokes equations but results in a model having different constants from the standard k-ε with additional terms and functions in the transport equations for k and ε.

$$\frac{\partial}{\partial t}(pk) + \frac{\partial}{\partial x_i}(pku_i) = \frac{\partial}{\partial x_j}\left(\alpha_k \mu_{eff}\frac{\partial k}{\partial x_j}\right) + G_k + G_b - \rho\epsilon - Y_M + S_k \tag{6}$$

$$\frac{\partial}{\partial t}(p\epsilon) + \frac{\partial}{\partial x_i}(p\epsilon u_i) = \frac{\partial}{\partial x_j}\left(\alpha_\epsilon \mu_{eff}\frac{\partial \epsilon}{\partial x_j}\right) + C_{1\epsilon}\frac{\epsilon}{k}(G_k + C_{3\epsilon}G_b) - C_{2\epsilon}\rho\frac{\epsilon^2}{k} - R_\epsilon + S_\epsilon \tag{7}$$

G_k represents the generation of turbulence kinetic energy due to the mean velocity gradients, G_b is the generation of turbulence kinetic energy due to buoyancy, Y_M represents the contribution of the fluctuating dilation on compressible turbulence to the overall dissipation rate.
α_k and α_ε are the inverse effective Prandtl numbers for k and ε, while S_k and S_ε are user-defined constants. The RNG k-ε model within Ansys Fluent has an additional option to account for the effects of swirling flows by modifying the turbulent viscosity.

$$\mu_t = \mu_{t0} f\left(\alpha_s, \Omega, \frac{k}{\varepsilon}\right) \tag{8}$$

μ_{t0} is the turbulent viscosity without swirl modification and Ω is a characteristic swirl number. α_S is a swirl constant that can be modified depending on the swirl intensity being simulated. For mildly swirling flows, this value is set by default to 0.07, as in the case of the current study.

4. RESULTS AND DISCUSSION

4.1 Effect of sub-atmospheric pressure

For the simpler geometry model, at 101kPa the droplet diameter varied from 0 to 165μm with an SMD of 65μm. However, there is an extensive broadening of the droplet diameter range in the

sub-atmospheric cases, from 0-325μm to 0-475μm for 41kPa and 31kPa, respectively. This behaviour is similar to that reported by Caines et al. (2001), and can be observed in Tables 2 and 3, and by comparing Figs. 1, 10 and 11.

The resulting SMD for all pressure cases is significantly lower than that measured by Kozaily et al. (2009). This may be attributed to the introduction of a higher co-flow air velocity and the liner wall.

For the detailed geometry model, where the co-flow air is more realistically distributed, the SMD is in between the two previous cases. These results suggest that the spray SMD depends considerably on the AFR, for which the simpler model has the highest value.

The detailed model introduces less air into the combustion zone and therefore the local AFR is less than for the simple model. Kozaily's model has the lowest AFR since nearly all the air is introduced only through the atomizer. For all three models however, the SMD increases significantly with decrease in chamber pressure, agreeing with Jasuja and Lefebvre (1994), Caines et al. (2001) (Fig 1) and Rizkalla (1974) (Fig 4).

This was expected since the low air density at low pressures causes a reduction in the shear stresses, which results in poor atomization of the fuel liquid sheet. However, a decrease in air density should increase the fuel/air relative velocity near the injection point, providing a better atomization environment.

The fuel/air relative velocity however was kept constant at 28 m/s for all the simulations, which is a typical velocity at these sub-idle conditions. Kozaily et al. (2009) investigated the effect of different relative velocities on the spray SMD, showing how the SMD increases when the relative velocity decreases, especially at low atmospheric pressures.

Since the relative velocity was kept constant, the effect of having a low atmospheric pressure resulted in low density air, and therefore according to equation 2, this results in a decrease in the We number, hindering the atomization process. Since neither fuel properties, nor air velocities were changed during the simulations, the other parameters in equation 2 are constant.

The droplet distribution of the three different models, for the 101, 41 and 31kPa operating pressures simulated, are illustrated in Figs. 12-14, respectively. These show clearly how the distribution is highly dependent on the operating pressure. The differences in the results between each model can be attributed to two factors. First, the co-flow air velocity in Kozaily's model was assumed to be 1m/s in order to neglect the effect of surrounding air, since the main focus was to analyze the fuel spray of the airblast atomizer only.

Additionally, no proper liner wall was modelled, thus not confining the air and fuel within a small space as they would be in a real combustor environment.

Table 2 SMD (μm) results from various studies.

Case study	101kPa	41kPa	31kPa
Caines et al. (2001)	70	150	180
Kozaily et al. (2009)	100	220	300
Simple geo	65	143	205
Complex	80	213	267

Table 3 Droplet size (μm) range results from various studies.

Case study	101kPa	41kPa	31kPa
Caine et al. (2001)	0-150	0-350	0-400
Kozaily et al. (2009)	0-200	0-475	0-775
Simple geo	0-165	0-325	0-475
Complex	0-165	0-375	0-575

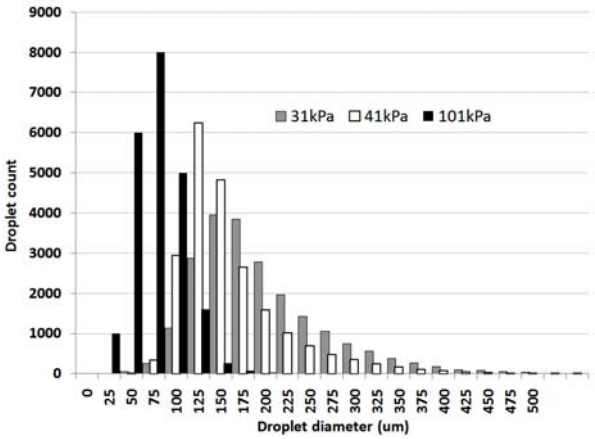

Fig.10 Fuel droplet distribution for detailed model.

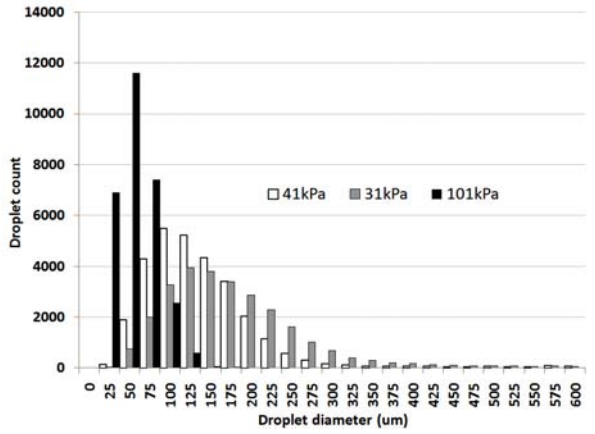

Fig. 11 Fuel droplet distribution for baseline simple model.

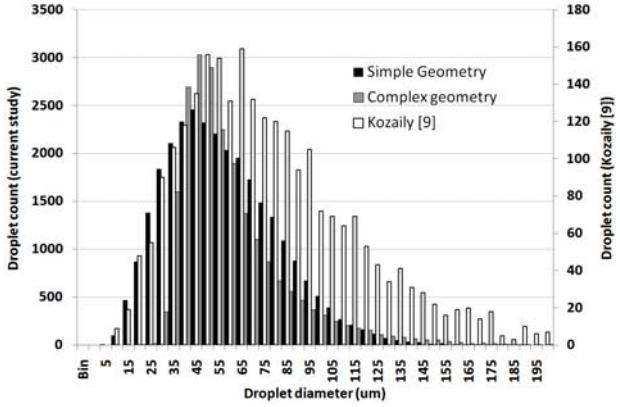

Fig.12 Fuel droplet distribution at 101kPa.

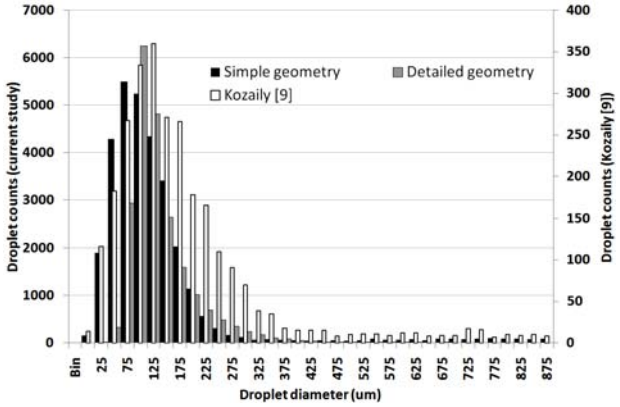

Fig. 13 Fuel droplet distribution at 41kPa.

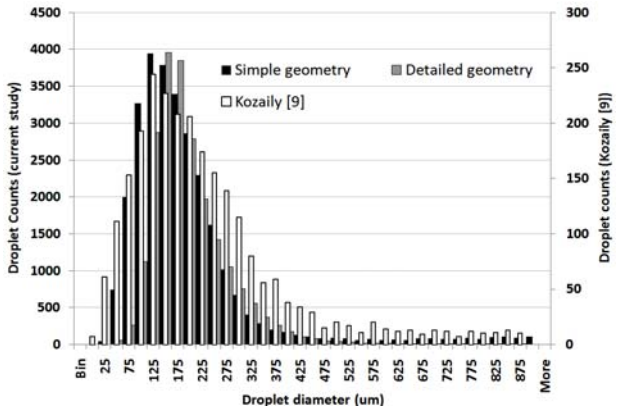

Fig. 14 Fuel droplet distribution at 31kPa.

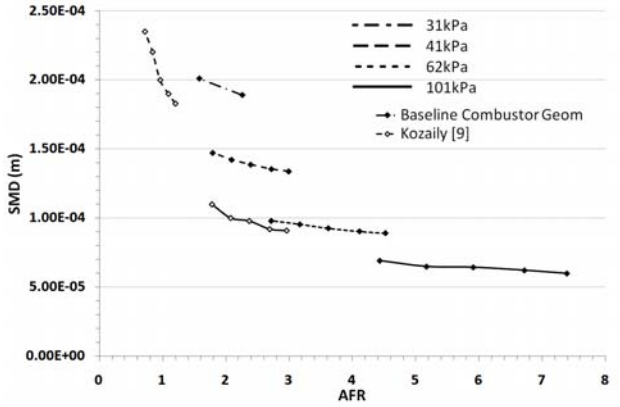

Fig. 15 Fuel droplet distribution at 31kPa.

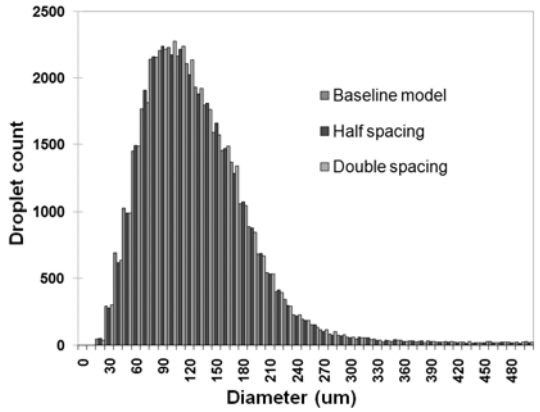

Fig. 16 Fuel droplet distribution (41kPa).

The co-flow air used in the current study considerably raises the shear stress forces on the fuel liquid sheet and the AFR. By including the liner wall, the fuel/air mixture was confined in a defined volume, increasing the stresses between fuel and air.

In considering the air-to-fuel ratio, Fig. 15 shows how significant the AFR is when operating at low chamber pressures. These results show the same tendency as the experimental work by Jasuja (1984) illustrated in Fig. 3.

4.2 Effect of chamber volume

The variation of chamber volume was defined by the spacing between the liner walls and the atomizer in the simple combustor model.

The main aim was to compare the differences in fuel spray structures generated by different chamber volumes under sub-idle conditions (101kPa, 41kPa and 31kPa) whilst keeping the fuel flow rate constant at 12g/s.Results for the 41kPa case are shown in Fig. 16.

The size of the chamber does not seem to influence the droplet distribution. Similar results were obtained for the 101 and 31kPa cases.

4.3 Droplet velocity, residence time and penetration

For the simple geometry combustor model, the fuel particles maintain higher velocities at atmospheric conditions, compared to the 41kPa case as shown in Fig. 17 and 18. Similar observations were made by Kozaily et al. (2009) and in the detailed model. In terms of the residence time, Kozaily's results indicate a significant number of droplets with a high residence time, distributed along the entire volume of the spray cone (Fig. 19).

This is probably due to the low co-flow air simulated, which does not help the particles travel further downstream into the combustor. In

contrast, the detailed and simplified model results (Figs. 20 and 21) indicate that the droplets with the highest residence times are found further downstream, since they are aided by the higher velocity co-flow air.

The velocity and residence time are also reflected in the penetration levels measured. Results by Kozaily et al. (2009) and the simple model simulations indicate a higher penetration level by the droplets at atmospheric conditions.

At sub-atmospheric pressures, penetration is reduced by 40-45% according to Kozaily et al. (2009), and by 20% according to the simple combustor model.

As regards the variation of the particle penetration level in different geometries simulated in this study, it was observed at 101kPa that this is dependent on the spacing between the liner wall and the atomizer.

The baseline model shows less penetration at 101kPa than Geometry 2 (Figs. 22 and 23). This may be due to the design configurations of the liner wall, as the farthest particle penetration was in Geometry 2 at 101KPa, which has the smallest volume.

At sub-atmospheric conditions, this behaviour was not observed due to the non-uniform distribution of the fuel/air mixture and all the geometries have quite similar fuel penetration levels.

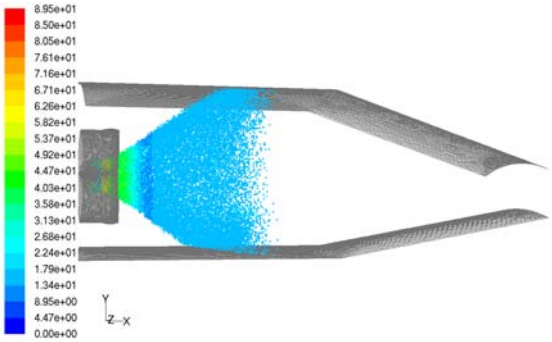

Fig. 17 Geometry 1: Velocity magnitude (m/s) at 101kPa.

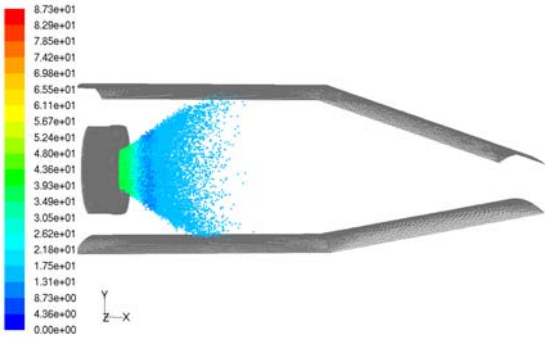

Fig. 18 Geometry 1: Velocity magnitude (m/s) at 41kPa.

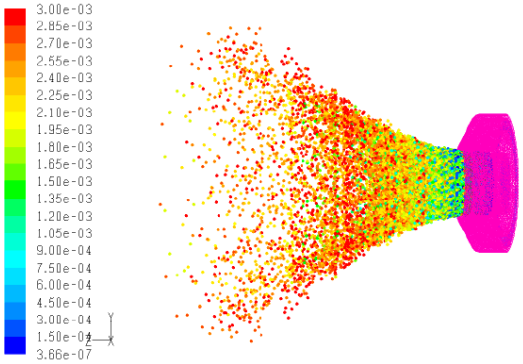

Fig. 19 Residence time (s) at 41kPa (Kozaily et al. 2009).

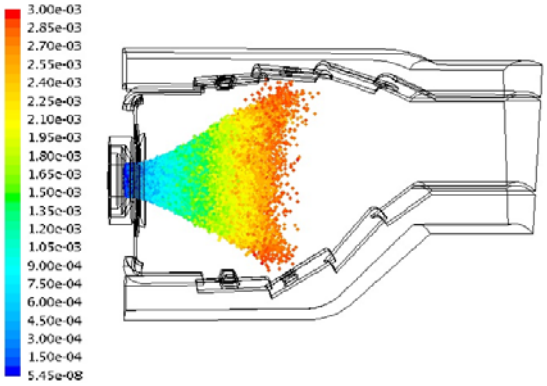

Fig. 20 Detailed model: residence time (s) at 101kPa.

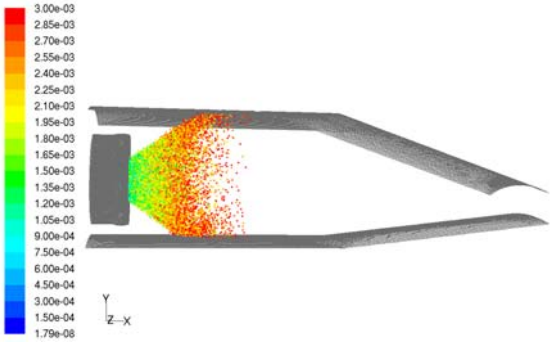

Fig. 21 Geometry 1: Residence time (s) at 41kPa.

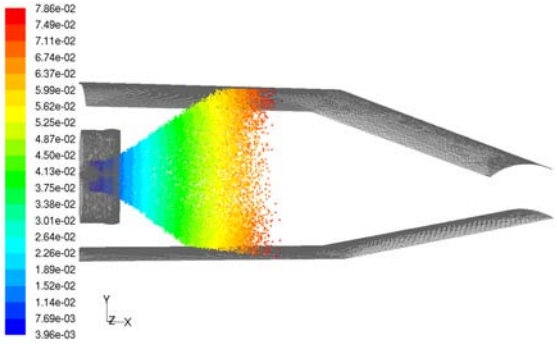

Fig. 22 Baseline model: Fuel penetration (m) at 101kPa.

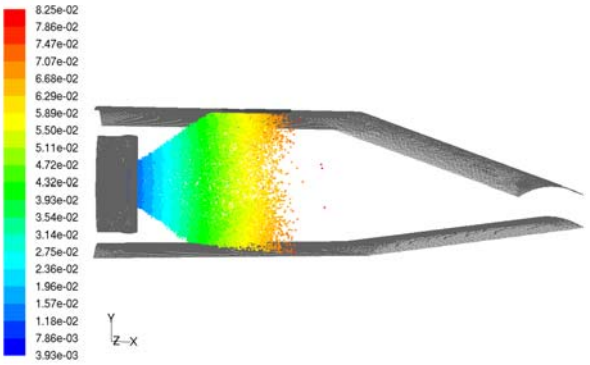

Fig. 23 Geometry 2: Fuel penetration (m) at 101kPa.

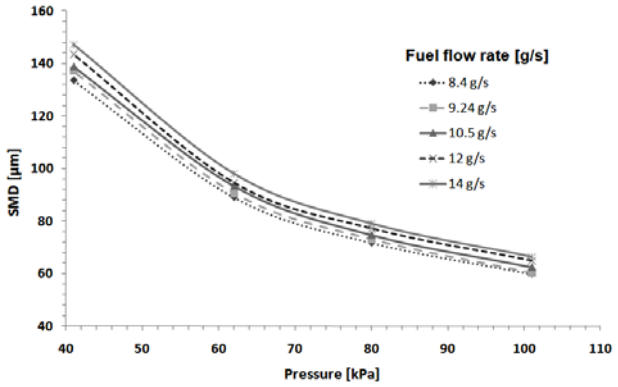

Fig. 24 Baseline model: SMD vs operating pressure at different fuel flow rates.

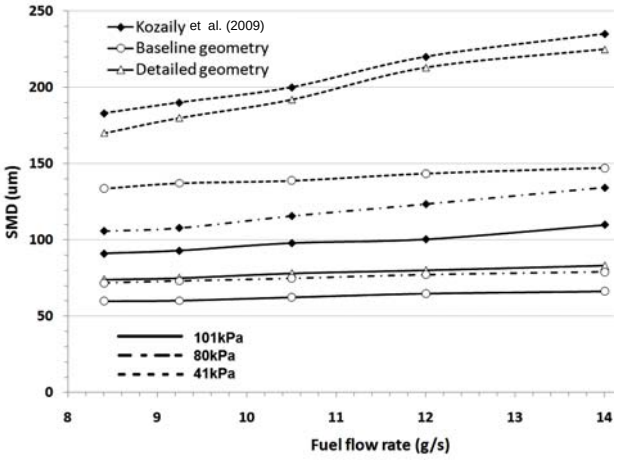

Fig. 25 SMD vs. fuel flow for various operating pressures.

4.4 Effect of fuel flow rates

Results from the baseline model (Fig. 24) indicate that at 101kPa and 80kPa, the change in fuel flow rate slightly affects the SMD of the fuel droplets, unlike at low pressures where the effect is more pronounced. Reduction in chamber pressure rapidly increases the SMD due to poor atomization of the droplets. The increase in fuel flow rates at these conditions further deteriorates the atomization and mixing processes due to further reduction in AFR. This reduction in air momentum per unit of mass fuel reduces the degree of atomization. Similar behaviour is observed for the other models (Fig. 25), where the 41kPa case consistently gives higher SMD values over the entire range of fuel flow rates simulated.

5. CONCLUSIONS

The objective of this work was to analyse, using CFD, the behaviour and performance of an airblast atomizer, under various sub-atmospheric conditions. Numerical CFD models were built in FLUENT for this goal. Unfortunately, there is very little experimental data available to verify the outcomes of these simulations.
The results were compared with experimental work by several independent researchers as well as CFD simulations, in order to assess what differences may arise, when the airblast atomizer operates at a typical low power condition within an aero gas turbine:

- The droplet size distribution of the combustor geometries shows a wide increase at sub-atmospheric pressures compared to idle. SMD was also found to increase by a factor of about 2 at 41kPa and by a factor of 3 at 31kPa, when compared with the 101kPa condition. This trend was also observed by Caines et al. (2001).
- In comparison with Kozaily's results, a reduction in both droplet size distribution and SMD were observed. This reduction is mainly due to the co-flow air, which increased radically the AFR. A reduction in SMD of about 35% and 20% at idle and 30% and 11% at 31kPa was observed for the simple geometry and detailed geometry models, respectively.
- The detailed geometry spray simulations gave SMDs, which are between those of the simpler geometry and Kozaily's. These results show the effect of the amount of co-flow introduced into the chamber, which directly changes the local AFR, on which the SMD is dependent at low pressures.
- No significant change in droplet size distribution and spray SMD were observed when models of different liner wall diameters were simulated. This may be due to the high AFR imposed because of the large amount of co-flow air injected.
- Droplet penetration seems to be dependent on the liner wall geometry only at atmospheric conditions but irrelevant at sub-idle conditions.

- An increase in fuel flow results in higher values of SMD both at idle and sub-idle conditions. However the effect is much more significant at sub-idle conditions.
- The actual velocity through the atomizer is not constant throughout the sub-idle operating regime of the engine, and therefore a more accurate model would have different inlet velocities for each condition simulated. This analysis and a study of the flow field behaviour at low mass flows will be presented in future publications.

NOMENCLATURE

ρ_A	Air density
d_0	Droplet diameter
U_R	Relative air velocity
σ	Liquid surface tension
η_{ce}	Evaporation rate-limited combustion efficiency
P_3	Combustor inlet pressure
V_C	Total combustion zone volume (pre-dilution)
λ_{eff}	effective value of evaporation constant
T_C	Combustion zone temperature
f_C	Fraction of total combustor air employed in combustion
m_A	Air mass flow rate

Abbreviations

AFR	Air to fuel ratio (by mass)
CFD	Computational Fluid Dynamics
RANS	Reynolds Averaged Navier Stokes
SFC	Specific Fuel Consumption
SMD	Sauter Mean Diameter

REFERENCES

1. ANSYS (2009). *Fluent 12.0 Theory Guide*, Ansys Inc.
2. Beck J, Lefebvre A., Koblish T (1989). Airblast atomization at conditions of low air velocity. *AIAA 27th Aerospace Sciences Meeting*, Reno, USA.
3. Caines BN, Hicks RA, Wilson CW (2001). Influence of sub-atmospheric conditions on the performance of an airblast atomiser. *AIAA/ASME/SAE/ASEE 37th Joint Propulsion Conference and Exhibit*, Salt Lake City, USA.
4. Chalet D, Chesse P (2010). Analysis of unsteady flow through a throttle valve using CFD. *Engineering Applications of Computational Fluid Mechanics* 4(3):387-395.
5. Datta A, Som SK (1999). Effects of spray characteristics on combustion performance of a liquid fuel spray in a gas turbine combustor. I*nternational Journal of Energy and Research* 23:217-228.
6. Gjesing R, Hattel J, Fritsching U (2009). Coupled atomization and spray modelling in the spray forming process using openFoam. *Engineering Applications of Computational Fluid Mechanics* 3(4):471-486.
7. Jasuja AK (1979). Atomization of crude and residual fuel oils. *Journal of Engineering for Power* 101(2):250-258.
8. Jasuja AK (1984). Effects of airblast atomizer design upon spray quality. *AGARD Conference Proceedings No.353 entitled Combustion Problems in Turbine Engines*.
9. Jasuja AK, Lefebvre AH (1994). Influence of ambient pressure on drop-size and velocity distributions in dense sprays. *Symposium on Combustion* 25(1):345-352.
10. Kozaily J, Zachos PK, Pachidis V, Singh R (2009). Gas turbine fuel atomization dynamics under sub-atmospheric conditions. ISABE 2009-1160, Montreal, Canada.
11. Lefebvre A.H (1985). Fuel effects on gas turbine combustion – ignition, stability, and combustion efficiency. Transactions of ASME, *Journal of Engineering for Gas Turbines and Power* 107.
12. Lefebvre AH (1989). *Atomization and Sprays*. Hemisphere Publishing Corporation, Taylor and Francis, London.
13. Lefebvre AH (1998). *Gas Turbine Combustion*. 2nd ed. Taylor and Francis, London.
14. Manzar MA, Shah SN (2009). Particle distribution and erosion during the flow of Newtonian and non-Newtonian slurries in straight and coiled pipes. *Engineering Applications of Computational Fluid Mechanics* 3(3):296-320.
15. Orme M (1997). Experiments on droplet collisions, bounce, coalescence and disruption. *Progress in Energy and Combustion Science* 23:65-79.
16. Parsons JA, Jasuja AK (1986). Effect of air pressure upon spray angle/width characteristics of simplex pressure swirl atomizers. ASME. *31st International Gas*

Turbine Conference and Exhibit, Düsseldorf, Germany.
17. Reitz RD (1987). Mechanisms of atomization processes in high-pressure vaporizing sprays. *Atomization and Spray Technology* 3:309-337.
18. Rizkalla AA (1974). *The Influence of Air and Liquid properties on Airblast Atomization*. PhD Thesis. Cranfield University, School of Engineering.
19. Rizkalla AA, Lefebvre AH (1975). The Influence of Air and Liquid Properties on Airblast Atomization. *Journal of Fluid Engineering* 97(3):316-320.
20. Sheen HJ, Chen WJ, Jeng SY, Huang TL (1996). Correlation of swirl number for a radial-type swirl generator. *Experimental Thermal and Fluid Science* 12:444–451.
21. Tu J, Yeoh GH, Liu C, (2008). *Computational Fluid Dynamics – A Practical Approach*. Butterworth-Heinmann, Elsevier.
22. Zachos PK, Grech N, Charnley B, Pachidis V, Singh R (2011). Experimental and numerical investigation of a compressor cascade at highly negative incidence. *Engineering Applications of Computational Fluid Mechanics* 5(1):26-36.